

# Synthesis and size evolution of 1D hydroxyapatite crystals under surfactant-free hydrothermal conditions

C García-Negrete<sup>1</sup>, R Gómez<sup>2</sup>, L Brun<sup>1</sup>, M Barrera<sup>2</sup>, G Arteaga<sup>1</sup>, A Beltrán<sup>3</sup>, and A Fernández<sup>3,4</sup>

<sup>1</sup>Facultad de Ciencias e Ingenierías, Universidad del Sinú, Montería, Colombia

<sup>2</sup>Departamento de Química, Universidad de Córdoba, Montería, Colombia

<sup>3</sup>Escuela Politécnica Superior, Universidad de Sevilla, Sevilla, España

<sup>4</sup>Instituto de Ciencia de Materiales de Sevilla, Consejo Superior de Investigaciones Científicas, Sevilla, España

E-mail: carlogarcian@unisinu.edu.co

**Abstract.** Hydroxyapatite nanoparticulate materials have received a great deal of scientific attention due to their dental and orthopedic applications but simple strategies to control particle characteristics (*e.g.*, surface area, shape and size distribution) are still needed. Among several hydroxyapatite structures, one-dimensional nanoscale materials such as nanowires, nanorods and nanobelts can be synthesized in the presence of specific surfactants added during synthesis in order to alter the particle growth. This contribution is aimed to explore strategies to obtain one dimensional hydroxyapatite crystals without the use of surfactants. Particularly, we study the effect of several variables such as temperature, reaction time and pH on shape and size of hydroxyapatite crystals produced under hydrothermal conditions. The results obtained show the formation of hydroxyapatite nanorods as well as some interesting insights about how to control particle sizes in samples obtained at temperatures between 180 °C and 220 °C. These results have potential benefits at the time of producing one dimensional hydroxyapatite crystals in a simple and not expensive way.

## 1. Introduction

Hydroxyapatite,  $\text{Ca}_{10}(\text{PO}_4)_6(\text{OH})_2$ , has been used for long time as bone graft substitute in dental and orthopedic applications due its biocompatibility and chemical composition similarity to bone and teeth in mammals [1-3]. Beyond its well-known biocompatibility, several characteristics (*e.g.*, surface area, shape and size distribution) make nanoparticulate hydroxyapatite a key functional material for several applications such as drugs delivery [4-6], protein purification [7,8] and cellular imaging [9,10]. On the other hand, one-dimensional (1D) nanoscale materials such as nanorods and nanobelts can be assembled into hierarchical structures like polyedra and clusters [11-13]. Hence, systematic constructions commonly produced through metallic assembly [14,15] can be produced from hydroxyapatite nanorods as building blocks.

Beside the aspects of hierarchical structures and building blocks assembly, the preparation of hydroxyapatite nanorods using simple and low-cost methods is also important to study. In this research, hydroxyapatite nanorods were produced through the use of a surfactant-free hydrothermal method. We particularly study changes in nanorod sizes when variables such as temperature, reaction time and pH



are modified in the hydroxyapatite synthesis. Results are shown about particle size shortening and broadening for hydroxyapatite particle design.

## 2. Experimental

Calcium nitrate tetrahydrate ( $\text{Ca}(\text{NO}_3)_2 \cdot 4\text{H}_2\text{O}$ ) and sodium hydrogen phosphate ( $\text{Na}_2\text{HPO}_4 \cdot 12\text{H}_2\text{O}$ ) were used to prepare aqueous solutions of  $\text{Ca}(\text{NO}_3)_2 \cdot 4\text{H}_2\text{O}$  and  $\text{Na}_2\text{HPO}_4 \cdot 12\text{H}_2\text{O}$  at 0.33 M and 0.11 M concentrations respectively; with a Ca/P atomic ratio of 1.67. Then, small amount of 1 M NaOH solution was added to each precursor solution to adjust the pH value to a defined value between 11 and 12. The solutions were mixed in a teflon vessel and placed in a steel autoclave. The mixture was allowed to react for established times. The as-obtained precipitates were washed several times with distilled water and finally with ethanol absolute. The obtained solids were then dried at 90 °C for 3 hours and storage in a desiccator for further characterizations. The prepared samples were characterized by X-ray diffraction (XRD; Panalytical Empyrean Alpha-1 operating with a Bragg-Brentano geometry) and transmission electron microscopy (TEM, FEI Talos F200S microscope operating at an accelerating voltage of 200 kV).

## 3. Results

### 3.1. XRD characterization

Figure 1 displays the XRD patterns of a typical sample prepared at pH 11 while temperature and reaction time were set at 200 °C and 8 hours respectively. XRD patterns were ascribed to a phase-pure hydroxyapatite (ICSD card. 98-002-2060, hexagonal, space group P63/m). Similar XRD results were obtained for the other samples. However, analysis of XRD patterns from the sample prepared at pH 12, while maintaining the same temperature and reaction time, evidenced the presence of carbonate apatite (data not shown) in addition to hydroxyapatite. Thus, pH 11 was chosen as a reference value for further experiments.

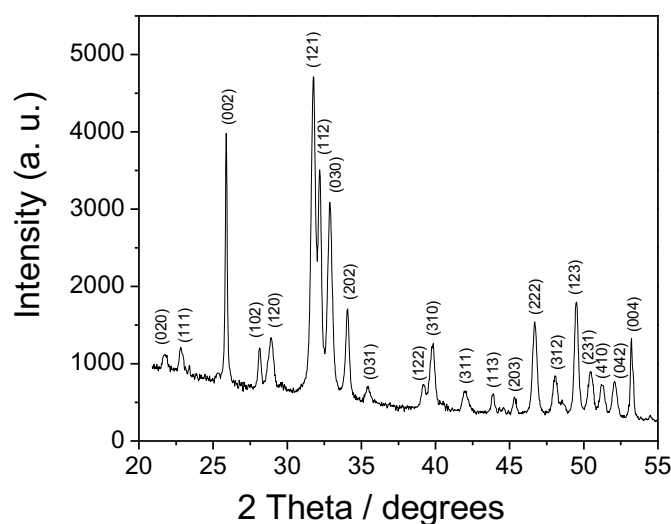


**Figure 1.** XRD patterns of a sample prepared at pH 11.

### 3.2. Effect of the reaction temperature

Morphology and particle sizes of samples obtained at different reaction temperatures were analysed through TEM analyses (Figure 2 to Figure 4). For comparison purposes, pH and reaction time were set at 11 and 8 hours respectively for all samples. TEM images of samples prepared at 180 °C, 200 °C and 220 °C are shown in Figure 2(a), Figure 3(a) and Figure 4(a) respectively. It was evidenced the formation of particles with rod-like shape in all cases. Therefore, synthetic procedures used are selective toward the formation of rods in spite of reaction temperatures used were between 180 °C and 220 °C.

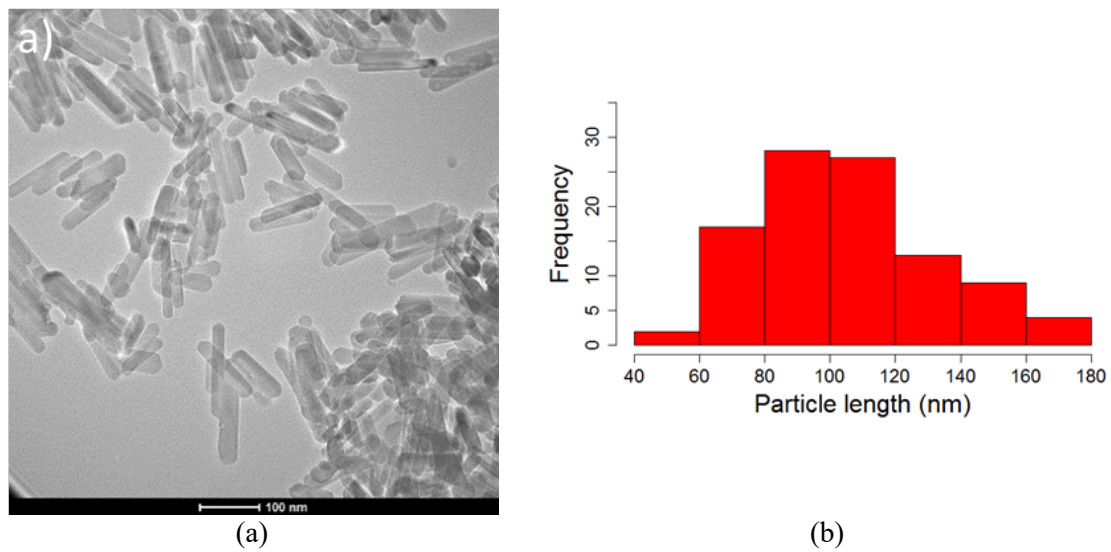


**Figure 2.** (a) TEM image of a sample prepared at 180 °C, (b) length size distribution.

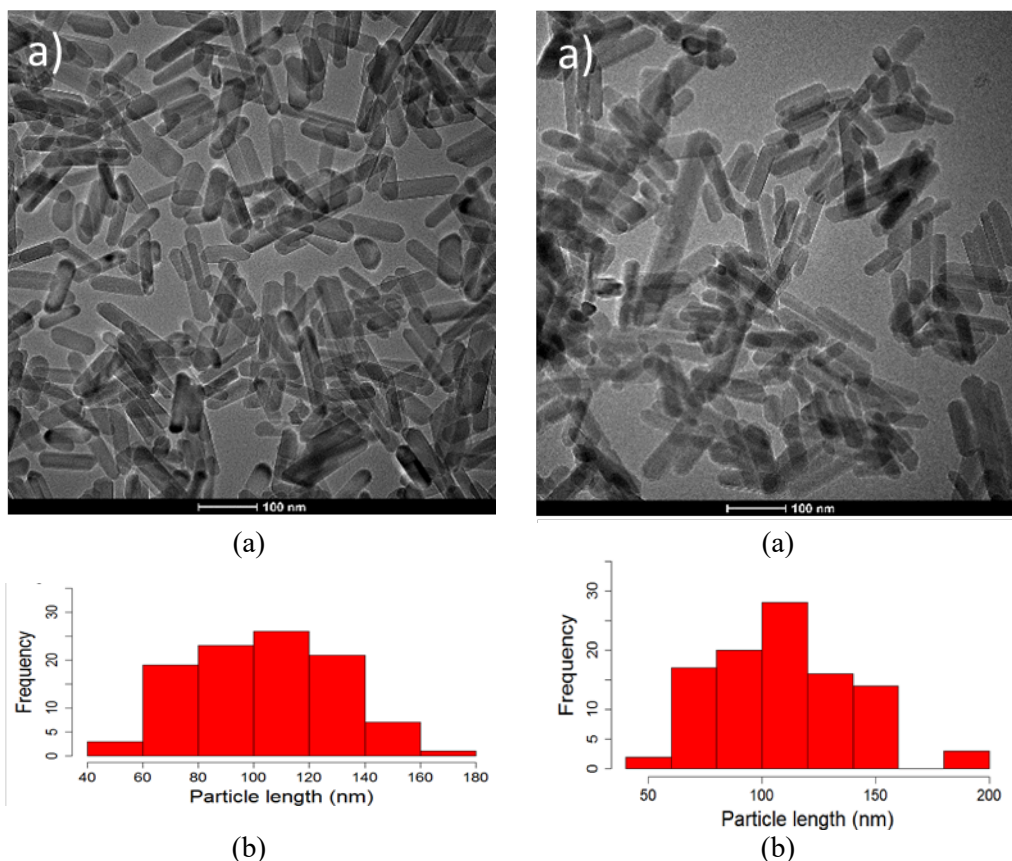


**Figure 3.** (a) TEM image of a sample prepared at 200 °C, (b) length size distribution.

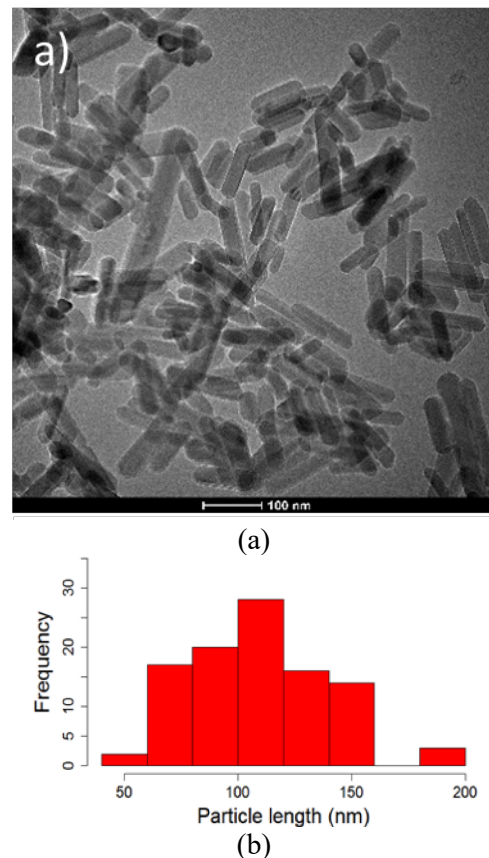


**Figure 4.** (a) TEM image of a sample prepared at 220 °C, (b) length size distribution.

Based on surfactant-free synthesis, other studies also reported the formation of 1D hydroxyapatite particles at quite similar reaction conditions but using another pH value [16,17]. In one case, rod-like shape particles were found at 200 °C [16] while in the other case, samples prepared at 180 °C and 200

°C were described as nanobelts [17], indicating the importance of correlating the different synthesis parameters. In this study, the effect of the reaction temperature is better evidenced on particle sizes. Length size distributions of samples prepared at 180 °C, 200 °C and 220 °C are shown in Figure 2(b), Figure 3(b) and Figure 4(b) respectively. For the sample prepared at 180 °C, the mean particle length was 102.2 ( $\pm 25.8$ ) nm. Then, as the reaction temperature increases to 200 °C, the particle length was 103.9 ( $\pm 26.6$ ) nm. Previous studies [16,17] showed that 1D particles with length sizes larger than 150 nm are produced at 200 °C but using another pH value. Finally, as the reaction temperature increases to 220 °C, the particle length was 108.1 ( $\pm 29.3$ ) nm. These results evidenced a simple trend, specifically, the particle length tends to be higher with the temperature increases.

### 3.3. Effect of the reaction time

In this section, the particle size evolution of hydroxyapatite samples prepared at different reaction time is discussed. For comparison purposes, pH and reaction temperature were set at 11 °C and 200 °C respectively. Figure 5 depicted the mean particle length of samples thermally treated for 8, 12 and 24 hours. For the sample treated for 8 hours, mean particle length was 103.9 ( $\pm 26.6$ ) nm. Interestingly, when the reaction time increases to 12 hours, the mean particle length decreases to 84.7 ( $\pm 37.3$ ) which suggests a partial dissolution of matter at nanorod tips leading to a particle length shortening. Later, when the reaction time increases to 24 hours, the mean particle length also increases to 130.1 ( $\pm 51.3$ ) nm. This second process can be seen as a lateral growth on rods, leading to the particle widening. In fact, as revealed in Figure 6, the mean particle width increases with the time for all increments tested. After reaction for 8 hours, the mean particle width was 25.6 ( $\pm 5.77$ ) nm. As the reaction time increased to 12 hours, the mean particle width was 28.9 ( $\pm 7.24$ ) nm. Finally, the mean particle width was 31.9 ( $\pm 10.25$ ) nm after reaction for 24 hours. The Ostwald ripening effect, where small crystals dissolve in order to feed the growth of larger ones, is known in colloid systems [18]. This situation is quite similar to the results found in this section, where initially, a dissolution of matter takes place in order to feed a further growth of particles.

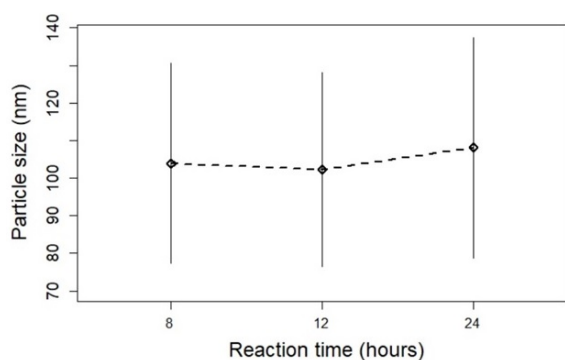


**Figure 5.** Mean particle length for nanorods obtained at different reaction times.

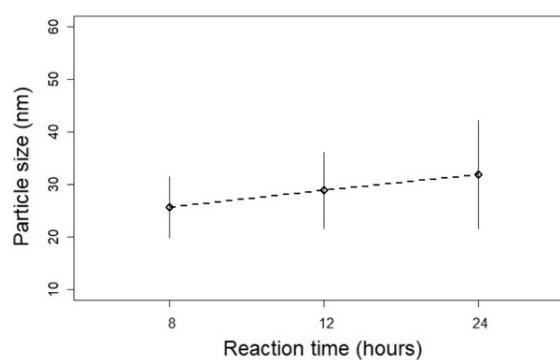


**Figure 6.** Mean particle width for nanorods obtained at different reaction times.

## 4. Conclusions

Well crystallized hydroxyapatite nanorods have been produced herein through a surfactant-free hydrothermal method. Variable such as reaction temperature and reaction time showed to have effect over particle sizes. Hydroxyapatite nanorods were obtained with lengths between 102.2 nm and 108.1 nm for temperatures between 180 °C and 220 °C. Although 8 hours was a good reaction time to produce well crystallized nanorods, when hydrothermal reaction is performed for 12 hours the mean particle length initially decreases due to a matter dissolution however the particle length again increases after reaction for 24 hours due to a further growth. Overall, these results represent suitable insights for hydroxyapatite particle design.

## References

- [1] Okada M and Matsumoto T 2015 *Japanese Dental Science Review* **51** 85
- [2] Yelten-Yilmaz A and Yilmaz S 2018 *Ceramics International* **44** 9701
- [3] García C, García C and Paucar C 2012 *Inorganic Chemistry Communications* **20** 90
- [4] Lee W-H, Loo C-Y and Rohanizadeh R 2019 *Materials Science and Engineering: C* **99** 929
- [5] Benedini L, Placente D and Ruso J 2019 *Materials Science and Engineering: C* **99** 180
- [6] Babaei M, Ghaee A and Nourmohammadi J 2019 *Materials Science and Engineering: C* **100** 874
- [7] Chen G, Zhitomirsky I and Ghosh R 2019 *Talanta* **199** 472
- [8] Itoh D, Yoshimoto N and Yamamoto S 2019 *Current Protein & Peptide Science* **20** 75
- [9] Zhang K, Zeng K, Shen C, Tian S and Yang M 2018 *Microchimica Acta* **185** 225
- [10] Vázquez-Hernández F, Mendoza-Acevedo S, Mendoza-Barrera C, Mendoza-Álvarez J and Luna-Arias J 2017 *Materials Science and Engineering: C* **71** 909
- [11] Yu Y-D, Zhu Y-J, Qi C and Wu J 2017 *Journal of Colloid Interface Science* **496** 416
- [12] Zhao S-N, Yang D-L, Wang D, Wang J-X and Chen J-F 2019 *Journal of Materials Science* **54** 3878
- [13] Yu Y-D, Zhu Y-J, Qi C and Wu J 2017 *Ceramics International* **43** 6511
- [14] García-Negrete C, Rojas T, Knappett B, Jefferson D, Wheatley A and Fernández A 2014 *Nanoscale* **6** 11090
- [15] García-Negrete C, Knappett B, Schmidt F, Rojas T, Wheatley A Hofer F and Fernández A 2015 *RSC Advances* **5** 55262
- [16] Li H, Mei L, Liu H, Liao L, Kumar R 2017 *Crystal Growth & Design* **17** 2809
- [17] An L, Li W, Xu Y, Zeng D, Cheng Y and Wang G 2016 *Ceramics International* **42** 3104
- [18] Boyjoo Y, Pareek V and Liu J 2014 *Journal of Materials Chemistry A* **2** 14270